Mapping the CD4 Binding Domain of gp17, a Glycoprotein Secreted from Seminal Vesicles and Breast Carcinomas[†]

Stéphane Basmaciogullari,[‡] Monica Autiero,[§] Raphaël Culerrier,[‡] Jean-Claude Mani,[∥] Muriel Gaubin,[‡] Zohar Mishal,[⊥] John Guardiola,[§] Claude Granier,[∥] and Dominique Piatier-Tonneau*,[‡]

Génétique Moléculaire et Biologie du Développement, ERS 1984, Centre National de la Recherche Scientifique, 19 rue Guy Moquet, 94801 Villejuif, France, International Institute of Genetics and Biophysics, Consiglio Nazionale della Ricerche, via Marconi 10, 80125 Naples, Italy, Immunoanalyse et Innovation en Biologie Clinique, UMR 9921, Centre National de la Recherche Scientifique, 15 avenue Charles Flahault, 34060 Montpellier, France, and UPS 47, Centre National de la Recherche Scientifique, 19 rue Guy Moquet, 94801 Villejuif, France

Received October 14, 1999; Revised Manuscript Received January 31, 2000

ABSTRACT: gp17, a secretory CD4-binding factor isolated from the human seminal plasma, is identical to the gross cystic disease fluid protein-15, a specific marker for primary and metastatic breast tumors. We previously demonstrated that gp17 binds to CD4 with high affinity and strongly inhibits T lymphocyte apoptosis induced by sequential cross-linking of CD4 and T cell receptor (TCR). To further characterize the gp17/CD4 interaction and map the gp17 binding site, we produced a secreted form of recombinant gp17 fused to human IgG1 Fc, gp17-Ig. We showed that gp17-Ig exhibits a binding affinity for CD4 similar to that of native gp17. As no information about gp17 structure is presently available, 99 overlapping gp17 peptides were synthesized by the Spot method, which allowed the mapping of two CD4 binding regions. Alanine scanning of CD4-reactive peptides identified critical residues, selected for site-directed mutagenesis. Nine gp17-Ig mutants were generated and characterized. Three residues within the carboxy-terminal region were identified as the major binding domain to CD4. The Spot method combined with mutagenesis represents a refined approach to distinguish the contact residues from the ones contributing to the conformation of the CD4-binding domain.

The gp17 glycoprotein is secreted at elevated concentrations (0.5−1 mg/mL) in the human seminal plasma of healthy individuals (*1*). It has been shown to specifically bind to the D1-D2 region of CD4 (*1*), a T cell surface molecule involved in the immune response (*2*). The partial amino acid sequence of gp17 (*3*), and the cloning of gp17 cDNA from a seminal vesicle library (*4*) have revealed that this protein is identical to a factor already known as gross cystic disease fluid protein-15 (GCDFP-15) (*5*) or prolactin-inducible protein (PIP) (*6*, *7*), expressed in benign and malignant breast tumors. Identity has also been found (*3*) with the secretory actin-binding protein (SABP), isolated from human seminal plasma (*8*, *9*) and with the extra parotid glycoprotein (EP-GP) secreted in the saliva (*10*, *11*). The gp17/GCDFP-15/PIP/SABP/EP-GP protein has been detected in a number of normal exocrine organs such as the bronchial epithelium, the sweat, salivary and lacrimal glands, in the seminal vesicles, and secreted in their corresponding fluids (*1*, *7*, *8*, *11*, *12*). Moreover, it is expressed in gross cystic disease, in breast cancers exhibiting apocrine features, and in metastasis of mammary origin (*12*−*18*). The role of gp17/GCDFP-15/PIP/SABP/EP-GP in physiological conditions as well as in tumoral pathology is presently unknown.

The finding that gp17 binds to CD4 with high affinity (*1*, *19*) has led to the examination of possible interference of gp17 with CD4-mediated functions. In addition to its role as a coreceptor in antigen recognition of peptides associated with MHC[1] class II proteins (*2*), CD4 acts as a signal-transducing molecule during T-cell activation by its association with the protein tyrosine kinase $p56^{lck}$ (*20*) and also serves as the primary cellular receptor for HIV-1 retroviruses (*21*, *22*). The binding of the viral envelope glycoprotein gp120 to CD4 mediates attachment of HIV-1 particles which enter the cells through other non-CD4 cellular receptors recently identified (reviewed in ref *23*). We have demonstrated that gp17 is able to partially inhibit the binding of gp120 to CD4 and the formation of syncytia between cells

[†] This work was supported by Centre National de la Recherche Scientifique (CNRS), France, by grants from Association pour la Recherche sur le Cancer (ARC) and from Fondation de France to DPT. S.B. is a fellow from ARC, and M.A. is a fellow from the European Union (BIO2-CT94-7520 and BIO-CT98-5025) and EMBO, successively. Research in J.G. laboratory is supported by AIRC.

* To whom correspondence should be addressed. Phone: +33 1 49 58 35 06. Fax: +33 1 49 58 35 09. E-mail: piatier@infobiogen.fr.

[‡] Génétique Moléculaire et Biologie du Développement.

[§] International Institute of Genetics and Biophysics.

[∥] Immunoanalyse et Innovation en Biologie Clinique.

[⊥] UPS 47.

[1] Abbreviations: AP, alkaline phosphatase; BSA, bovine serum albumin; ELISA, enzyme-linked immunosorbent assay; FACS, fluorescein-activated cell sorter; FITC, fluorescein isothiocyanate; Fmoc, *N*-(9-fluorenyl)methoxycarbonyl; HIV-1, human immunodeficiency virus type 1; MHC, major histocompatibility complex; PAGE, polyacrylamid gel electrophoresis; PBS, phosphate-buffered saline; PCR, polymerase chain reaction; SDS, sodium dodecyl sulfate; TCR, T cell receptor; TRITC, tetramethyl-rhodamin isothiocyanate.

10.1021/bi992398l CCC: $19.00
Published on Web 04/13/2000

expressing CD4 and HIV-1 envelope protein (*19*). Furthermore, gp17 has been found to be a strong inhibitor of T lymphocyte apoptosis induced by sequential cross-linking of CD4 and TCR (*24*). The anti-apoptotic effect of gp17 is restricted to this apoptosis pathway and is associated with a moderate, but significant increase of the expression of the anti-apoptotic proto-oncogene Bcl-2 (*24*). These results emphasize the need to determine the gp17 regions involved in CD4 binding in order to define the functional parts of this glycoprotein.

In the present study, we have examined the effects of mutations introduced into the gp17 sequence on the interaction between gp17 and CD4. A two-step approach has been developed: first, alanine scanning of gp17-derived peptides (*25*, *26*) allowed the rapid identification of two sets of residues located in the amino- and carboxy-terminal region of gp17, contributing to CD4 binding; then, in vitro site-directed mutagenesis was used to create mutations of the selected residues. A new mammalian production system has been designed leading to the secretion of recombinant wild-type and mutant gp17 molecules fused to the human IgG1 Fc portion. The association of the two methods allowed the identification of gp17 residues which are involved in CD4 binding and those important for the conformation of the CD4-binding site.

MATERIALS AND METHODS

Proteins, Antibodies, and Reagents. Native gp17 was purified from pooled seminal plasma of healthy donors by affinity chromatography on chicken anti-gp17 polyclonal antibodies coupled to CNBr-activated Sepharose-4B (Pharmacia, Uppsala, Sweden). Chicken polyclonal antibodies were raised against gp17, as described (*24*). Recombinant soluble CD4 molecule containing the four extracellular domains (sCD4) (*27*) and recombinant IgG3-CD4 immunoadhesin comprising CD4 domains 1 and 2 (*28*) were kindly provided by R. Sweet (Smith Kline Beecham Pharmaceuticals, King of Prussia, PA) and A. Traunecker (Institute for Immunology, Basel, Switzerland), respectively. sCD4 used in BIACORE experiments was from Repligen (Needham, MA). Monoclonal antibodies (mAbs) were obtained from commercial sources: anti-human IgG1 and FITC-conjugated anti-CD4 (OKT4) mAbs were from PharMingen (San Diego, CA) and Ortho Diagnostics Systems (Raritan, NJ), respectively. Secondary Abs were HRP- and FITC-conjugated goat anti-human IgG (Fc specific) and anti-chicken Ig, TRITC-conjugated rabbit anti-chicken Ig, alkaline phospatase (AP)-conjugated goat anti-mouse and rabbit anti-chicken Ig (Sigma, St-Louis, MO). Human IgG was purchased from Rockland (Gilbertsville, PA).

Synthesis of gp17 Peptides on Cellulose Membranes. The general protocol of Spot multiple peptide synthesis (*25*) has been described previously (*26*). Membranes were obtained from Abimed (Langenfeld, Germany). Fmoc amino acids and *N*-hydroxybenzotriazole were from Novabiochem (Meudon, France). An ASP222 robot (Abimed) was used for the coupling steps. All peptides were acetylated at their N-terminus. After the peptides sequences were assembled, the side-chain protecting groups were removed by trifluoroacetic acid treatment.

Protein Labeling and Binding Assays with Cellulose-Bound Peptides. IgG3-CD4 (5 μg) was iodinated using the chloramine T method, as described (*29*). The specific activity was 4×10^8 cpm/μg. Cellulose membranes with wild-type and Ala-substituted gp17 peptides were incubated in 12 mL of binding buffer [TBS-T (5 mM Tris, pH 7, 15 mM NaCl, 0.27 mM KCl, 0.05% Tween 20), 10% saccharose, Blocking Buffer (Genosys, Cambridge, U.K.)] containing 5×10^6 cpm/mL ^{125}I-labeled IgG3-CD4 for 1 h and 30 min at 37 °C. After extensive washing in TBS-T, the membranes were autoradiographied for 2 h with Scientific Imaging Film (Kodak, Rochester, NY). Spot intensity was determined with the Molecular Analyst software after scanning autoradiographs. The stripping of the membranes was achieved by successive treatment with 1% SDS, 8 M urea, 12.7 mM 2-mercaptoethanol, and 10% acetic acid, 50% methanol.

Alternatively, membranes were incubated with binding buffer containing chicken anti-gp17 Ab for 1 h and 30 min at 37 °C then with AP-conjugated rabbit anti-chicken Ig Ab for 1 h and 30 min at 37 °C. Binding was revealed by addition of AP substrate (5-bromo-4-chloro-3-indolyl phosphate-3-(4,5-dimethyltriazol-2-yl)-2,5-diphenyltetrazolium bromid, Sigma) giving a blue precipitate. A dimethyl formamide washing step was performed before the stripping protocol described above.

Construction of Recombinant spIg-gp17 Plasmids and in Vitro Site-Directed Mutagenesis. The mammalian expression plasmid spIg (R&D Systems Europe Ltd., Oxon, U.K.) was used to clone gp17 sequence encoding the mature protein. A gp17 cDNA fragment (nucleotides 121−474) (*4*) was amplified by PCR using the High Fidelity Pwo DNA polymerase (Roche Molecular Biochemicals, Meylan, France), and primers were designed according to manufacturer specifications. The 5′ primer (5′-ACTGGGATCCGCAG-GACAACACTCGGAAGATC-3′) started from the codon encoding the gp17 amino acid 29 and contained a *Bam*HI restriction site (underlined) present in CD33 signal sequence (*30*); the 3′ primer (5′-ACTGGGATCC**ACTTACCTGT**TTC-TACCTTTAGGATTTCAAT-3′) ended with the codon upstream from the stop codon and contained a splice donator site (bold) and a *Bam*HI restriction site (underlined). The amplified fragment was cloned into pCR2.1 (pCR2.1-gp17) using the TA cloning Kit (Invitrogen, Groningen, The Netherlands) and sequenced according to the standard molecular biology techniques (*31*). The *Bam*HI restriction fragment was tranferred into spIg (spIg-gp17); control sequencing of the insert/vector junctions was carried out.

gp17-Ig mutants were prepared by encoding the desired mutation in overlapping 35-mer oligonucleotides (Genosys). These primers were used in a PCR reaction with the pCR2.1-gp17 construct as template using the QuickChange site-directed mutagenesis kit (Stratagene, La Jolla, CA). After amplification of mutant pCR2.1-gp17 plasmids, the *Bam*HI restriction fragments were subcloned into spIg; confirmation of the presence of the mutation was achieved by sequencing.

Expression, Purification of recombinant gp17-Ig, and SDS−PAGE Analysis. COS-7 cells (10^7) grown in DMEM-Glutamax (Life Technology, Cergy Pontoise, France) supplemented with 10% fetal calf serum (FCS), penicillin (100 IU/mL) and streptomycin (100 μg/mL), were transfected by electroporation with 5 μg of recombinant gp17 plasmids and 15 μg of pUC18 carrier DNA. Cells were harvested 48 h after transfection for immunofluorescence staining and flow cytometry analysis. Alternatively, they were allowed to grow

for 5 days after transfection in Protein Free Hybridoma Medium II (Life Technology) supplemented with penicillin, streptomycin, and 2 mM L-glutamine before culture supernatant was harvested for purification of secreted gp17-Ig. COS cells were also transfected with pcDNA3-gp17 containing the whole gp17 cDNA (*4*) or cotransfected with pcDNA3-gp17 and pcDNA3-CD4.

Secreted gp17-Ig was purified by affinity chromatography on protein A Sepharose-4B (Pharmacia) following the specifications of the manufacturer. The concentration of purified gp17-Ig preparations was determined with the Micro BCA Protein Assay Kit (Pierce, Rockford, IL). The samples were analyzed by 10% SDS−PAGE and silver staining. Western blots were carried out by electrotransfer to polyvinylidene fluoride (PVDF) membrane (Roche Molecular Biochemicals). Membranes were blocked in 0.1% Tween 20, and 5% nonfat dry milk PBS and incubated with anti-gp17 Ab then with HRP-conjugated anti-chicken Ig Ab or with HRP-conjugated anti-human IgG (Fc specific) Ab (Sigma). Blots were developed by the enhanced chemiluminescence technique (Amersham Pharmacia Biotech, Buckinghamshire, U.K.) as instructed by the manufacturer.

Immunofluorescence, Flow Cytometry, and Confocal Microscopy Analysis. Transfected cells were analyzed for gp17-Ig synthesis 48 h after electroporation. Cells were trypsinized, washed in cold PBS, and fixed/permeabilized by cold 70% ethanol for 2 h on ice. After washing in cold PBS containing 0.1% BSA (PBS−BSA), cells were incubated for 1 h with FITC-conjugated goat anti-human IgG (Fc specific) antibody, washed in PBS, and analyzed with a FACS Vantage flow cytometer (Becton Dickinson, San Jose, CA).

For confocal microscopy analysis, cells were seeded in Lab-Tek chambers (Nunc, Naperville, IL) 24 h after transfection and cultured for a further 24 h. Fixation and permeabilization of adherent cells were performed by successive incubations with 4% paraformaldehyde and 0.1% Triton X-100. After washing in PBS−BSA, cells were stained successively with chicken anti-gp17 Ab and FITC- or TRITC-conjugated anti-chicken Ig Ab. An additional staining with FITC-conjugated OKT4 mAb was performed for COS cells cotransfected with pcDNA3-gp17 and -CD4. Nuclei were counterstained with propidium iodide when indicated. Labeled specimens were scanned with an ACAS 570 Interactive Laser Cytometer (Meridian Instruments, Inc., Okemos, MI). Sections were taken every 1 μm, and the images shown are the calculated projections of all sections.

ELISA Analysis of Recombinant gp17-Ig interactions with anti-gp17 Ab and CD4. Binding assays were performed at 37 °C in 96-well microtiter plates (Dynatech, Billingshurst, U.K.) coated with various receptors. Wells coated with native gp17, wild-type gp17-Ig, or human IgG (20 nM in PBS) were successively incubated with various dilutions of chicken anti-gp17 Ab in PBS containing 0.1% Tween 20 (PBS-T) for 1 h, then with AP-conjugated rabbit anti-chicken Ig Ab for 30 min. Wells coated with anti-human IgG1 mAb (50 nM) were successively incubated with various dilutions of gp17-Ig or human IgG in PBS-T for 1 h, chicken anti-gp17 Ab (1:3000) for 1 h, and AP-conjugated rabbit anti-chicken Ig Ab (1:3000) for 30 min. Wells coated with sCD4 were successively incubated with various dilutions of wild-type and mutant gp17-Ig or human IgG in PBS-T for 2 h, anti-human IgG1 mAb for 1 h, and AP-conjugated goat anti-mouse Ig Ab for 30 min. The AP substrate was *p*-nitrophenyl phosphate disodium (Sigma), and the absorbance was measured at wavelength 405 nm.

Real-Time Analysis of Native and Recombinant gp17 binding to Immobilized CD4 Using BIACORE. Studies were performed at 25 °C using BIACORE (Biacore AB, Uppsala, Sweden). Recombinant soluble CD4 molecules (Repligen) (50 μg/mL) in 10 mM sodium acetate, pH 5, were immobilized onto a sensor chip CM5 (*32*) activated with 100 mM *N*-ethyl-*N*′-(3-dimethylaminopropyl) carbodiimide hydrochloride/400 mM hydroxysuccinimide (EDC:NHS). The binding kinetics of native and recombinant gp17 molecules to CD4 were determined by injecting various concentrations of analyte in HBS buffer (Biacore AB), pH 7.4, at a flow rate of 30 μL/min. Dissociation was observed in HBS without dissociating agents at 30 μL/min. Kinetic parameters were determined using BIAevaluation 3.0 software (Biacore AB). The dissociation rate constants k_d and the association rate constants k_a were determined by the global method (*33*).

RESULTS

Production and Characterization of Secreted Recombinant gp17 in Transiently Transfected COS Cells. Production of recombinant gp17 (rgp17) was required for the mapping by mutagenesis of gp17 residues involved in CD4 binding. Transfection of COS cells with gp17 cDNA cloned into pCDNA3 did not allow to detect rgp17 in the cell culture supernatant, and only low amounts of rgp17 could be immunoprecipitated from the cell lysate (data not shown). Analysis of gp17 transfected COS cells by confocal microscopy revealed that rgp17 was efficiently expressed but remained confined in a compartment next to the nuclei, probably the endoplasmic reticulum and the Golgi apparatus (Figure 1A). No rgp17 was detected at or nearby the cytoplasmic membrane. As gp17 binds to CD4, we examined whether the coexpression of CD4 could influence rgp17 intracellular localization. Confocal microscopy analysis of COS cells cotransfected with recombinant CD4 and gp17 pCDNA3 plasmids (Figure 1B) showed that the colocalization of CD4 and rgp17 was restricted to the endoplasmic reticulum (yellow colored). Conversely, CD4 molecules were also detected at the cytoplasmic membrane (green colored). This indicated that CD4 expression was not able to redirect rgp17 to the membrane.

To produce a secreted form of rgp17, we used the mammalian expression vector spIg, which is designed to code for fusion proteins with a C-terminal human IgG1 Fc region and to facilitate their secretion in the cell culture supernatant through the CD33 signal peptide. The gp17 cDNA was engineered by PCR and cloned into spIg. Sequencing of the recombinant spIg-gp17 indicated that the construct encoded a 370 amino acid polypeptide, containing 19 residues derived from CD33 signal peptide (*30*), the sequence of mature gp17 (118 amino acids), the hinge region (15 residues), and Fc tail of human IgG1 (217 residues). An additional Thr between the last gp17 and the first Ig amino acid was generated by the construction.

Forty-eight hours after transfection with spIg-gp17, COS cells expressed high amounts of gp17-Ig molecule, as detected by confocal microscopy analysis (Figure 1C). The intracellular distribution pattern of gp17-Ig significantly

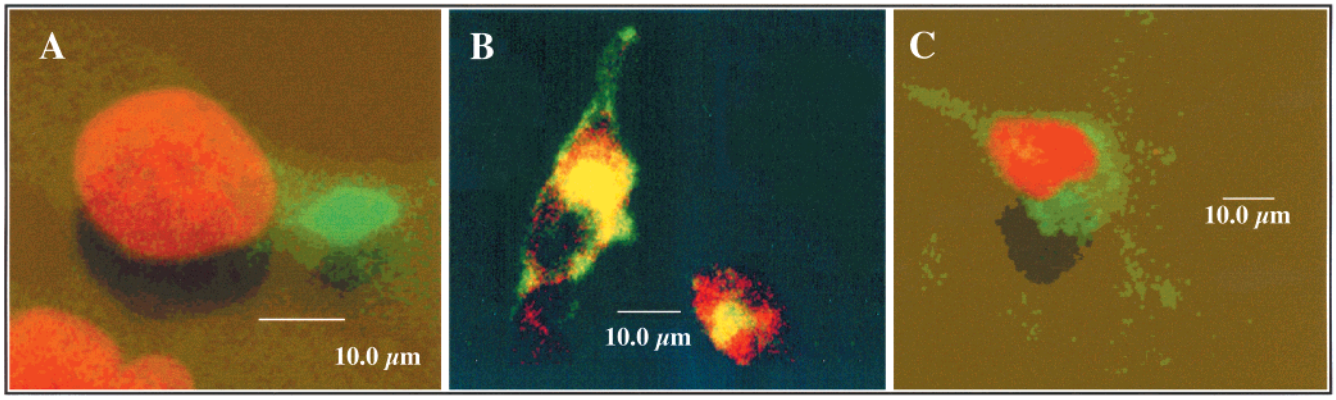

FIGURE 1: Intracellular localization of recombinant gp17 produced in transfected COS cells. Confocal microscopy analysis of COS cells transfected with gp17 cDNA cloned into pcDNA3 (A), with both gp17 and CD4 cDNA cloned into pcDNA3 (B), or with spIg-gp17 (C). Cells were fixed and permeabilized as described in the Materials and Methods and incubated with chicken anti-gp17 Ab (1:100) and FITC-conjugated goat anti-chicken Ig Ab (1:60) (A, C) or with FITC-conjugated OKT4 mAb (1:50) and chicken anti-gp17 Ab (1:100) and with TRITC-conjugated rabbit anti chicken Ig Ab (1:100) (B). Nuclei were stained with propidium iodide (5 μg/mL) immediatly prior to confocal microscopy analysis (A, C). 3D reconstruction of confocal sections are shown in panels A and C.

differed from that previously observed (Figure 1A) and the molecule was found inside the cytoplasm, thus suggesting that it can be targeted to the cell surface and secreted. COS cell culture supernatants were harvested 5 days after the transfection and gp17-Ig was purified by affinity chromatography on a protein A-Sepharose column. SDS−PAGE analysis of the eluted material revealed that secreted gp17-Ig exhibited an apparent molecular mass of 45 kDa under reducing conditions (Figure 2A). Under nonreducing condition gp17-Ig migrated as a 90 kDa form (Figure 2B, left panel). This form was recognized by anti-human IgG and anti-gp17 Abs by Western blotting (Figure 2B, middle and right panel, respectively), confirming that gp17-Ig dimerizes through disulfide bridges within the hinge region of the Fc portion, as expected.

Quantification of purified gp17-Ig showed that the average production efficiency was about 50 $\mu g/10^7$ transfected COS cells. The immunoreactivity of secreted WT gp17-Ig molecules was determined by ELISA using chicken anti-gp17 polyclonal Ab. As shown in Figure 2C, the binding of anti-gp17 Ab to immobilized gp17-Ig was higher than the binding to native gp17. This difference may be related to the 90 kDa dimeric form of gp17-Ig. The recognition pattern is specific for the gp17 part of the gp17-Ig molecule as demonstrated by the lack of anti-gp17 Ab binding to human IgG (Figure 2B, right panel, and Figure 2C).

To compare the reactivity of gp17-Ig and native gp17 glycoproteins with CD4, we used the BIACORE technology, which allows real-time analysis of molecular interactions. Various concentrations of recombinant and native gp17 were injected on immobilized recombinant CD4. The sensorgrams shown in Figure 3 revealed that native and recombinant gp17 bound efficiently to immobilized CD4. The determination of the kinetic parameters (dissociation and association rate constants k_d and k_a, respectively) of the binding reactions indicated that the kinetics of the binding of both molecules to CD4 fitted with a one-site model. The association and dissociation rates exhibited close values and the apparent equilibrium dissociation constants ($K_D = k_d/k_a$) of the two preparations were 5.98 and 10.4 nM for native gp17 and gp17-Ig, respectively (Figure 3). These data indicate that the recombinant gp17-Ig molecule has a binding affinity for CD4 close to that of the native protein and, therefore, represents a suitable tool for introducing mutations and studying their effects on the interaction with CD4.

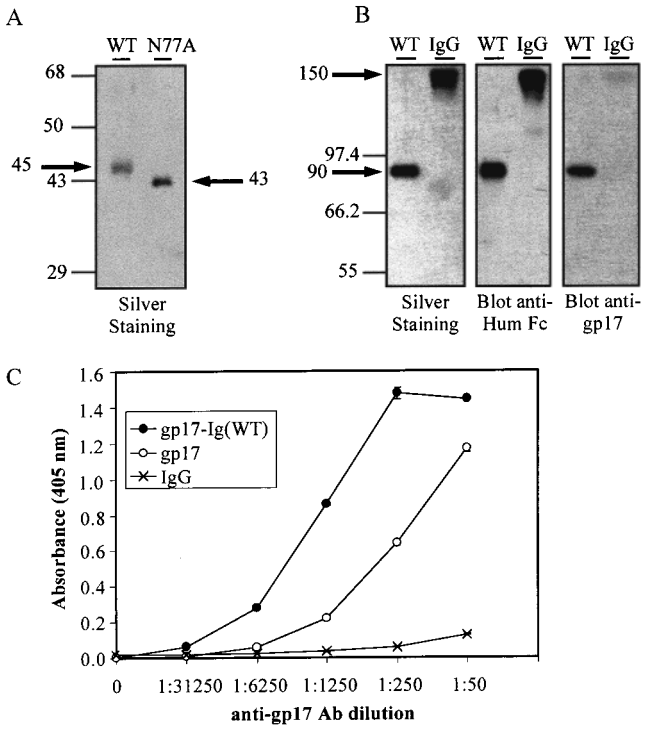

FIGURE 2: Structural characterization of gp17-Ig purified from transfected COS cells supernatant. (A) 10% SDS−PAGE analysis under reducing conditions of wild-type (WT) and unglycosylated mutant (N77A) gp17-Ig molecules (100 ng) (arrows indicate the position of glycosylated and unglycosylated gp17-Ig). (B) 10% SDS−PAGE analysis under non reducing conditions and Western blot analysis of wild-type gp17-Ig and human IgG (200 ng) (left panel), immunoblotting using HRP-conjugated anti-human IgG Fc Ab (1:10000) (middle panel), or chicken anti-gp17 Ab (1:5000) and HRP-conjugated anti-chicken Ig Ab (1:10000) (right panel). (C) Binding of chicken anti-gp17 Ab to native gp17, wild-type gp17-Ig, and human IgG. Molecules were immobilized on microtiter plates (20 nM). Binding of increasing concentrations of chicken anti-gp17 Ab was monitored by ELISA. Secondary antibody was PA-conjugated goat anti-chicken Ig Ab (1:500).

Determination of gp17 Regions Involved in CD4 Binding by the Spot Method. The ability of gp17 sequences to bind CD4 was investigated by the Spot method. The gp17

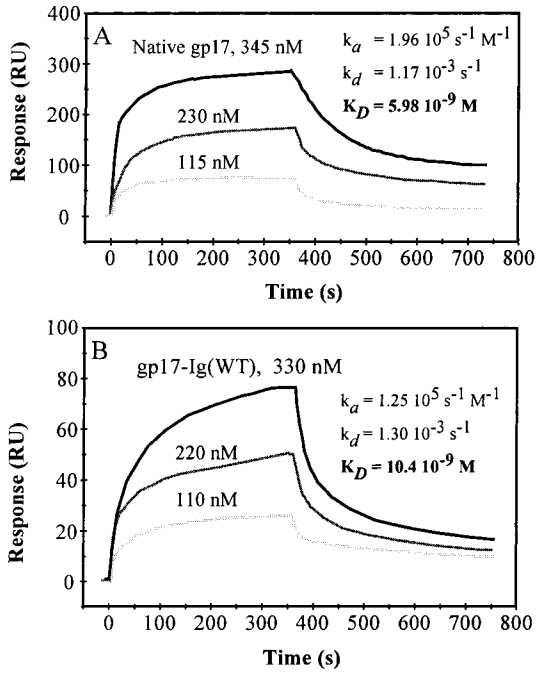

FIGURE 3: Surface plasmon resonance analysis of the interaction between immobilized CD4 and native and recombinant gp17. Various concentrations of soluble native gp17 [(A) 115, 230, and 345 nM] and gp17-Ig [(B) 110, 220, and 330 nM] were injected on a sensorship coated with sCD4. The rate constants k_a and k_d were determined using BIAevaluation 3.0 software.

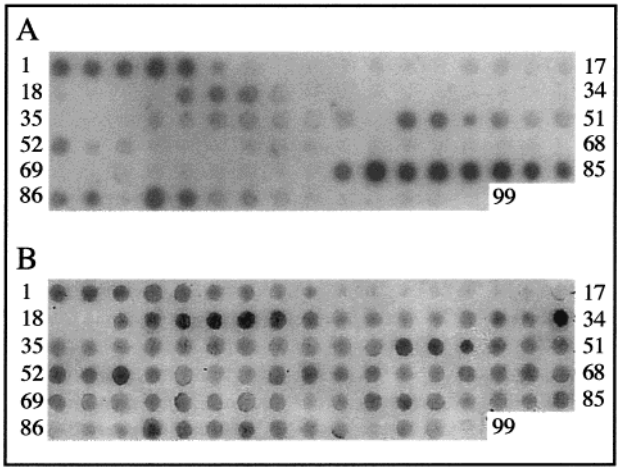

FIGURE 4: Reactivity of overlapping gp17 peptides with ^{125}I-labeled IgG3-CD4 and polyclonal anti-gp17 antibodies. The membrane on which the gp17 peptides were synthesized was incubated with ^{125}I-labeled IgG3-CD4 (12 mL, 5×10^6 cpm/mL) and processed for autoradiography (A), or with chicken anti-gp17 Ab (1:200) followed by AP-conjugated secondary Ab (1:1000) and AP substrate (B). Peptide numbers are indicated. Representative results of three independent experiments are shown.

sequence was represented as a set of 99 overlapping peptides of 20 residues each (one residue frameshift) on a cellulose membrane. The peptides were covalently bound to the membrane by their carboxy-terminal residues. Two β alanine residues served as a spacer between the cellulose and the first residue of the peptides to enhance the accessibility of a putative ligand for the carboxy-terminal part of the peptides. Incubation of the membrane with ^{125}I-labeled IgG3-CD4 (Figure 4A) revealed that 5 groups of peptides (peptides 1−5, 22−24, 46−48, 78−85, and 89−90) displayed a binding activity, albeit at variable extent. As measured by densitometry, peptides exhibiting the highest binding activity were located in the carboxy-terminal part of gp17 (peptides 78−85, group IV) (Table 1). A lower binding activity was observed for peptides 1−5 (group I) and 89−90 (group V). Identical results were obtained with ^{125}I-labeled recombinant sCD4 composed of the four extracellular domains of human CD4 (data not shown). The detection of IgG3-CD4 binding to membrane bound peptides was also studied by an indirect immunoenzymatic method using unlabeled IgG3-CD4 and AP-conjugated goat anti-human IgG Ab. An identical binding pattern was observed (data not shown). No binding of control human IgG3 to the peptides was detected (data not shown). Altogether, these results confirm that peptides 78−85 and to a lesser extent 1−5 and 89−90 specifically react with CD4.

Table 1: Sequences of gp17 Peptides and Their Reactivity for ^{125}I-Labeled IgG3-CD4[b]

Peptide number	Peptide sequence	Spot intensity [a]
	Group I	
1	QDNT**RKIIIKNFDIPKSVRP**	7,8
2	DNT**RKIIIKNFDIPKSVRP**N	6,9
3	NT**RKIIIKNFDIPKSVRP**ND	7,7
4	T**RKIIIKNFDIPKSVRP**NDE	10,7
6	KIIIKNFDIPKSVRPNDEVT	3,4
	Group II	
21	NDEVTAVLAVQTELKECMVV	<1
22	DEVTAVLAVQTELKECMVVK	6,5
23	EVTAVLAVQTELKECMVVKT	5,9
24	VTAVLAVQTELKECMVVKTY	4,6
25	TAVLAVQTELKECMVVKTYL	<1
	Group III	
45	ISSIPLQGAFNYKYTACLCD	<1
46	SSIPLQGAFNYKYTACLCDD	8,1
47	SIPLQGAFNYKYTACLCDDN	6,7
48	IPLQGAFNYKYTACLCDDNP	3,8
49	PLQGAFNYKYTACLCDDNPK	<1
	Group IV	
77	NRTVQIAAVVDVIRELGICP	<1
78	RTVQIAA**VVDVIRELGICPD**	8,6
79	TVQIAA**VVDVIRELGICPD**D	23,0
80	VQIAA**VVDVIRELGICPD**DA	14,4
81	QIAA**VVDVIRELGICPD**DAA	19,8
82	IAA**VVDVIRELGICPD**DAAV	17,5
83	AA**VVDVIRELGICPD**DAAVI	18,7
84	A**VVDVIRELGICPD**DAAVIP	13,3
85	**VVDVIRELGICPD**DAAVIPI	8,9
86	VDVIRELGICPDDAAVIPIK	4,7
87	DVIRELGICPDDAAVIPIKN	6,3
	Group V	
88	VIRELGICPDDAAVIPIKNN	<1
89	IRELGICPDDAAVIPIKNNR	10,6
90	RELGICPDDAAVIPIKNNRF	9,0
91	ELGICPDDAAVIPIKNNRFY	<1

[a] Spot intensity was measured with Molecular Analyst software. [b] The common epitope of the most reactive peptides are highlighted.

Most gp17 peptides were specifically recognized by polyclonal anti-gp17 Ab raised in chicken (Figure 4B). No binding was observed with the secondary antibody alone (data not shown). Some peptides exhibited a greater reactivity than others. The differences observed probably reflect the accessibility and/or immunogenicity of these regions in the native protein.

Identification of gp17 Residues Involved in CD4 Binding by Alanine Scanning. To identify the residues contributing to CD4 binding, alanine scanning of peptides 4 and 81 (see Table 1), which were among the most reactive peptides identified in the former assay, was performed. The binding of ^{125}I-labeled IgG3-CD4 to substituted peptides was quantified by densitometry (Figure 5). Single substitutions of Ala for Lys-6 and Lys-10 generated a 50% decrease in CD4

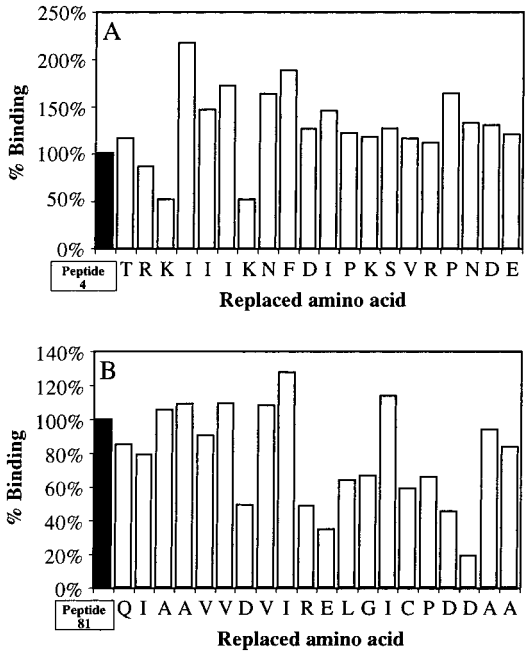

FIGURE 5: Determination of the residues contributing to the binding of IgG3-CD4 to gp17 peptides. (A) Alanine scanning of peptide 4. (B) Alanine scanning of peptide 81, native alanine residues were replaced by glycine. The membrane was incubated with ^{125}I-labeled IgG3-CD4 as described in Figure 3. Each bar represents the reactivity of the peptide whose sequence comprises an Ala substitution in place of the indicated amino acid. Black bars, wild-type peptides; open bars, substituted peptides. Representative results of two independent experiments are shown.

binding as compared to the wild-type peptide (Figure 5A). Ala substitutions for the other residues had no effect or enhanced CD4-binding activity of the peptide.

Alanine scanning of peptide 81, derived from gp17 region IV and exhibiting the strongest reactivity with CD4, allowed to identify five residues contributing to the gp17/CD4 binding (Figure 5B). Single substitution of Ala for Asp-87, Arg-90, Glu-91, Asp-97, and Asp-98 induced up to 80% of inhibition of CD4 binding, suggesting that these residues are important for the interaction with CD4. Replacement by Ala of Leu-92, Gly-93, Cys-95, and Pro-96 also decreased the binding of ^{125}I-labeled IgG3-CD4 but to a lesser extent. The other Ala substitutions did not affect CD4 binding. The contributing motif for the carboxy-terminal region may therefore be D_{87}- -$R_{90}E_{91}$- - - - -$D_{97}D_{98}$. It is noteworthy that all residues in the amino- and carboxy-terminal part of gp17 that appear to be involved in CD4 binding are charged amino acids, although not every charged residue was found to be involved.

Production of gp17-Ig Mutants by Site-Directed Mutagenesis. Mutations were introduced in gp17-Ig encoding cDNA as described in Materials and Methods. According to the results obtained with the Spot method, seven amino acids contributing to CD4 binding were replaced by an Ala residue. Ile-7 and Asp-23, which did not affect negatively CD4 binding (see Figure 5A), were also substituted with Ala. To control that functional glycosylation of wild-type and mutant gp17-Ig occurs in transfected COS cells, an additional mutation was created, consisting of Ala substitution for Asn-77 (N77A), which removes the unique glycosylation site in gp17. The secreted form of the gp17-Ig mutants was purified and quantified. SDS−PAGE analysis indicated that all mutants, but the N77A mutant, migrated as the wild-type (WT) gp17-Ig molecule (data not shown); the N77A mutant had an apparent molecular mass of 43 kDa (see Figure 2A), indicating that the N77A mutation prevented gp17-Ig glycosylation. These results confirm that gp17-Ig molecules are efficiently glycosylated in this production system. Most mutants were secreted in the culture supernatant as efficiently as WT gp17-Ig (1 μg/mL). However, two of them, K10A and N77A, were produced at a 4- and 10-fold lower concentration, respectively. The cytoplasmic expression level of K10A and N77A, as assessed by flow cytometry analysis of COS cells stained with a mAb specific for the IgG Fc tail 48 h after transfection, was similar to that of WT gp17-Ig (Figure 6) and the other mutants (data not shown), suggesting that mutations K10A and N77A affect the secretion process.

Effects of Mutations on gp17-Ig Binding to CD4. The binding to immobilized CD4 of the panel of gp17-Ig mutants was determined by ELISA (Figure 7, panels A and B). Mutations of residues in the N-terminal region of the protein did not reduce binding to CD4 (K6A) or it did poorly (K10A) (Figure 7A), in agreement with the finding that they did not cause a dramatic effect on the interaction of CD4 with gp17 peptides in the Spot assay. Conversely, the D87A, R90A, E91A, and D98A mutations, which severely affected CD4 binding to peptide 81, also abolished the binding of mutated gp17-Ig molecules to CD4 (Figure 7B). Only residue Asp-97 behaved in an unexpected fashion, as shown by the strong binding of the D97A gp17-Ig mutant to immobilized CD4 (Figure 7B). Surprisingly, two additional mutants in the N-terminal region, I7A and E23A, which did not decrease the binding of CD4 in Spot assays, also failed to bind to CD4 (Figure 7A).

ELISA analysis of the recognition of the gp17-Ig mutants by the polyclonal anti-gp17 Ab showed that all mutants but one exhibited the same pattern of reactivity as the wild-type gp17-Ig (Figure 7, panels C and D). By contrast, the molecule carrying the D98A substitution was not recognized by the anti-gp17 Ab (Figure 7D). This suggests that in D98A the epitopes recognized by the antibody may be hidden because of conformational changes.

It thus appears that while the behavior of mutations such as D87A, R90A, and E91A confirms that residues of the region of gp17 represented by peptide 81 (Table 1) are crucial for the CD4/gp17 interaction, other residues may also play an indirect role.

DISCUSSION

gp17, a protein secreted in the seminal plasma of healthy individuals (*1*) and identical (*3*, *4*) to GCDFP-15, PIP, SABP, and EP-GP (*5*, *6*, *8*, *10*), has been shown to bind to CD4 with high affinity (*1*, *19*). However, the functions of this CD4-binding factor remain unclear both in physiological and pathological conditions. Related to its high secretion level in the human seminal plasma (0.5−1 mg/mL) and colocalization with CD4-like molecules at the surface of spermatozoon (*34*), gp17 has been proposed to play a role in the fertilization processes based on CD4−MHC class II interactions (*34*). The observation that gp17 was able to block CD4-HLA-DR interaction (Autiero, unpublished results) has also suggested that gp17 may act as an immunomodulatory factor at insemination. However, the most striking in vitro function reported so far for gp17 is its strong inhibitory effect on T

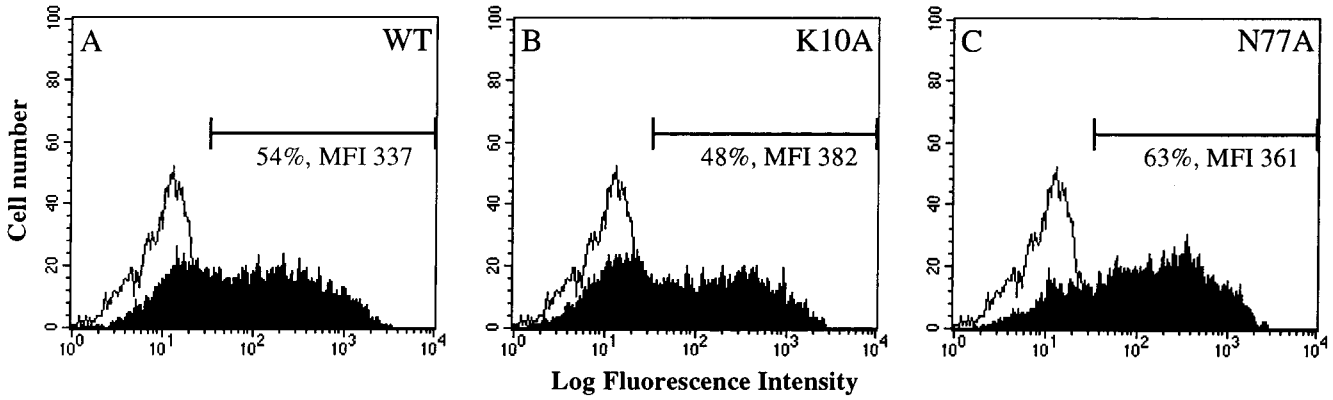

FIGURE 6: Flow cytometry analysis of intracytoplasmic WT and mutant gp17-Ig expression in transfected COS cells. COS cells were transiently transfected with recombinant spIg (black histograms) encoding WT gp17-Ig (A) and K6A and N77A mutants (B, C). Cells were fixed/permeabilized 48 h after transfection prior to staining with FITC-conjugated anti-human IgG mAb (Fc specifc) (1:100). Controls were COS cells transfected with spIg vector (white histograms). Percentages of labeled cells are indicated. MFI, mean fluorescence intensity.

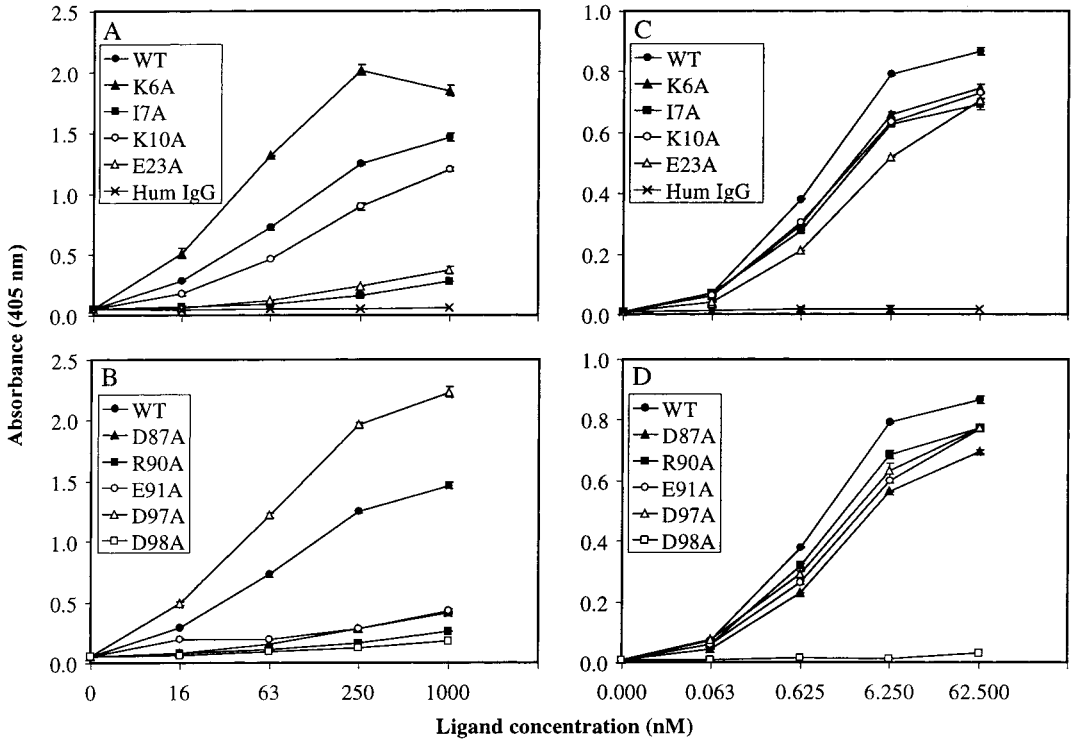

FIGURE 7: Wild-type and mutant gp17-Ig reactivity with CD4 and anti-gp17 Ab. (A, B) gp17-Ig molecules were incubated in microtiter plates coated with soluble CD4 (20 nM). gp17-Ig binding was detected by anti-human IgG1 (40 nM) and PA-conjugated goat anti-mouse Ig Ab (1:1000). (C, D) gp17-Ig molecules were incubated in microtiter plates coated with anti-human IgG Ab (50 nM). Chicken anti-gp17 Ab (1:3000) binding to gp17-Ig molecules was monitored with PA-conjugated goat anti-chicken Ig Ab (1:3000).

lymphocyte apoptosis induced by sequential activation of CD4 and TCR (*24*). The properties of gp17 to interfere with T lymphocytes signaling pathways are particularly interesting in regard to the behavior of tumor infiltrating lymphocytes in breast cancers which express gp17/GCDFP-15. Indeed, abnormal IL-2 secretion and signaling molecule expression have been reported in breast tumor infiltrating lymphocytes (*35*−*37*). However, the role of tumor-secreted gp17 in lymphocyte dysfunction in vivo remains to be elucidated.

To improve the characterization of gp17-CD4 interaction and to gain knowledge about gp17 regions and amino acids involved in CD4 binding, we report here the production of a new secreted form of recombinant gp17 and a combined analysis of the effects of point mutations within gp17 peptides and gp17 protein on gp17/CD4 interaction. We have demonstrated that two regions in the amino- and carboxy-terminal parts of gp17 are important for CD4 binding. Amino acids Asp-87, Arg-90, and Glu-91 most likely represent contact residues with CD4, while some others located both in the amino- and carboxy-terminal regions seem to play a role in the conformational integrity of the CD4-binding site.

Functional and structural studies have been limited up to date by the lack of available recombinant gp17 production systems. Attempts to produce rgp17 in bacterial expression systems (*3*, *38*) have been unsuccessful because the protein was invariably found in the inclusion bodies and methods for resolubilization and refolding were unsatisfactory. The expression of baculovirus-based vectors in insect cells has also led to the production of insoluble intracellular products (J.G., personal communication). More recently, successful production of soluble secreted rgp17 has been obtained in *P. pastoris* yeast (*39*). Since transient expression of proteins

by transfected COS cells usually yields high expression levels and is widely used in mutagenesis studies, we have analyzed the expression of rgp17 in these cells. We found that COS cells transfected with full-length gp17 cDNA cloned into pcDNA3 expressed high levels of rgp17. However, the protein stuck in the perinuclear compartment and was not secreted, as previously observed in HeLa cells transfected with a gp17-EGFP C-terminal fusion construct (*39*). Coexpression of CD4 with gp17 in double-transfected COS cells did not prevent gp17 retention, although CD4 clearly reached the cytoplasmic membrane. Conversely, COS cell transfected with spIg-gp17 construct led to the expression and secretion of about 5 μg of recombinant gp17-Ig/10^6 COS cells. These results indicate that the gp17 signal peptide does not support gp17 secretion by mammalian cell lines from epithelial origin. Its replacement by the CD33 signal peptide allowed the secretion of glycosylated gp17-Ig fusion protein. We have found that secreted gp17-Ig efficiently bound to CD4, as detected by ELISA, and exhibited an affinity for CD4 (K_D = 10.4 nM) near that of the native protein (K_D = 5.98 nM), as detected by BIACORE. Although, some structural variations between native gp17, which is found as tetramers in the seminal plasma (*3*), and the covalently linked dimeric gp17-Ig fusion protein may account for subtle binding affinity differences, gp17-Ig appears to be a suitable recombinant protein for mutagenesis studies.

As no information about gp17 structure is available to date, multiple peptide synthesis method has been used in order to identify the gp17 amino acids important for CD4 binding and to select mutations to be created in gp17-Ig. The Spot method (*25*) has proved to be a powerful tool to screen peptide ligand/receptor interactions (*40*, *41*). The reactivity of 99 20-mer membrane-bound peptides overlapping the whole gp17 sequence toward labeled CD4 allowed the identification of two regions of gp17 which bound CD4. These regions are located at the N-terminal end (residues 1−24, domain I) and within the C-terminal part (residues 78−104, domain IV) of gp17, suggesting that CD4 may bind to two distinct sites or that these two regions are spatially close in the folded protein. Peptides 4 and 81 belonging to domains I and IV, respectively, have been subjected to alanine scanning. Seven charged residues (Lys-6, Lys-10, Asp-87, Arg-90, Glu-91, Asp-97, and Asp-98) have been found to decrease CD4 binding when replaced by Ala. These residues have been selected for further in vitro site-directed mutagenesis studies and secreted gp17-Ig mutant molecules with Ala substitution have been produced by transfected COS cells. Two additional mutants have also been studied, I7A and E23A, which did not decrease CD4 binding in the spot assay. All mutants exhibited high intracytoplasmic expression levels, as detected with an antibody specific for the Fc tail. This indicates that mutations did not prevent gp17-Ig mutants synthesis by COS cells and suggests that no gross molecular distortion was generated. However, while all recombinant gp17-Ig molecules were efficiently secreted in the culture medium, the K10A mutant exhibited a low secretion level. This may be related to conformational changes interfering with the secretion process. Alternatively, mutations may generate molecular instability and increased sensitivity to degradation. A similar behavior was observed for the N77A mutant, which was created to suppress the unique glycosylation site of gp17 and used in this study to confirm that functional glycosylation of the other recombinant g17-Ig molecules occurs in COS cells.

The reactivity of mutant gp17 peptides and gp17-Ig molecules toward CD4 has been compared. Five mutations were found to decrease (K10A) or abolish (D87A, R90A, E91A, and D98A) the binding of gp17-Ig molecules to CD4. These results, in agreement with the low reactivity of the corresponding mutant peptides, emphasize the importance of these residues in gp17/CD4 interaction. However, the role played by these residues may differ. Residue Asp-98 appears to be involved in retaining the structural integrity of the gp17-Ig molecule rather than in establishing direct contact with CD4, as deduced from the lack of recognition of the D98A mutant by anti-gp17 Ab. A loss of reactivity due to ELISA conditions can be ruled out because gp17-Ig molecules were not directly adsorbed to plastic to avoid any possible denaturation. We thus suggest that the main gp17-binding motif to CD4 is D_{87}- -$R_{90}E_{91}$. The role of Lys-10 in the interaction of domain I with CD4 seems to be less stringent, as indicated by the 50% decrease and the weak reduction of CD4 binding to K10A peptide and K10A gp17-Ig, respectively. This suggests that, although Lys-10 is able to participate in CD4 binding, the presence of the unmodified carboxy-terminal region in the K10A gp17-Ig mutant is able to overcome Ala substitution for Lys-10 and thus to support CD4 binding. This observation reinforces the prominent role of the D_{87}- -$R_{90}E_{91}$ motif.

A second group of mutations has been characterized by their disparate effects on gp17/CD4 interaction, when expressed in gp17 peptides or gp17-Ig molecules. Mutations K6A and D97A decreased CD4 binding to peptides 4 and 81, while they were found to enhance the binding of the corresponding mutant gp17-Ig to CD4. Conversely, mutations I7A and E23A completely abolished gp17-Ig binding to CD4 whereas these residues were not considered as contributing residues according to the results of the alanine scanning of peptide 4. These discrepancies do not allow to consider that residues Lys-6, Ile-7, Glu-23, and Asp-97 directly bind to CD4. More probably, these mutations may generate conformational changes in gp17-Ig molecules either enhancing (K6A and D97A) or abolishing (I7A and D23A) their binding to CD4. Similarly, in the 20-mer peptides which can adopt secondary structure, substitutions of these residues may influence the accessibility of neighbor contact residues, such as Lys-10 in peptide 4, Asp-87, Arg-90, or Glu-91 in peptide 81. Unfortunately, the lack of monoclonal antibodies specific for gp17 did not allow to characterize in more details conformational changes induced by mutations. Altogether, these results emphasize the need of various approaches in order to interpret more confidently mutagenesis studies, which represent necessary but transient steps preceding crystal structure data in order to define active regions in a molecule.

In this regard, recombinant wild-type and mutant gp17-Ig molecules will be useful tools to explore further the functions of this glycoprotein, which remain elusive both in physiological and pathological conditions. Mutants which have lost their ability to bind CD4 will allow to dissect the intracellular signaling pathways depending on gp17/CD4 interaction, the mechanisms of the anti-apoptotic activity of gp17 (*24*), and more generally the role of this CD4-binding factor in host defense against infections and tumors.

In conclusion, the combined use of the Spot method and in vitro site-directed mutagenesis studies appears to be a useful approach to determine residues involved in ligand/receptor interactions. We clearly demonstrate that the D_{87}- -$R_{90}E_{91}$ motif in gp17 is the main CD4 interacting region. In addition, the production by transfected COS cells of secreted recombinant gp17-Ig glycoprotein exhibiting the same CD4-binding features as the native gp17 purified from seminal plasma constitutes a promising model for further crystal structure determination of this protein.

ACKNOWLEDGMENT

We thank Prs. Ray Sweet and André Traunecker for their generous supplies of recombinant soluble CD4 molecules. We are also grateful to Drs. M. Auroux and J. C. Soufir for providing seminal plasma samples.

REFERENCES

1. Autiero, M., Abrescia, P., and Guardiola, J. (1991) *Exp. Cell Res. 197*, 268−71.
2. Janeway, C. A. (1989) *Immunol. Today 10*, 234−8.
3. Autiero, M., Cammarota, G., Friedlein, A., Zulauf, M., Chiappetta, G., Dragone, V., and Guardiola, J. (1995) *Eur. J. Immunol. 25*, 1461−4.
4. Autiero, M., Bouchier, C., Basmaciogullari, S., Zaborski, P., El Marhomy, S., Martin, M., Guardiola, J., and Piatier-Tonneau, D. (1997) *Immunogenetics 46*, 345−8.
5. Haagensen, D. E., Jr., Mazoujian, G., Dilley, W. G., Pedersen, C. E., Kister, S. J., and Wells, S. A., Jr. (1979) *J. Natl. Cancer Inst. 62*, 239−47.
6. Shiu, R. P. C., and Iwasiow, B. M. (1985) *J. Biol. Chem. 260*, 11307−13.
7. Murphy, L. C., Tsuyuki, D., Myal, Y., and Shiu, R. P. C. (1987) *J. Biol. Chem. 262*, 15236−41.
8. Akiyama, K., and Kimura, H. (1990) *Biochim. Biophys. Acta 1040*, 206−10.
9. Schaller, J., Akiyama, K., Hess, D., Affolter, M., and Rickli, E. E. (1991) *Eur. J. Biochem. 196*, 743−50.
10. Rathman, W. M., Van Zeyl, M. J., Van den Keybus, P. A. M., Bank, R. A., Veerman, E. C. I., and Nieuw Amerongen, A. V. (1989) *J. Biol. Buccale 17*, 199−208.
11. Schenkels, L. C., Schaller, J., Walgreen-Weterings, E., Schadee-Eestermans, I. L., Veerman, E. C., and Amerongen, A. V. N. (1994) *Biol. Chem. Hoppe-Seyler 375*, 609−15.
12. Haagensen, D. E., Jr., and Mazoujian, G. (1986) in *Diseases of the Breast.* (Haagensen, C. D., Ed.) pp 474−500, W. B. Saunders Co., Philadelphia.
13. Murphy, L. C., Lee-Wing, M., Goldenberg, G. J., and Shiu, R. P. C. (1987) *Cancer Res. 47*, 4160−4.
14. Wich, M. R., Lillemoe, T. J., Copland, G. T., Swanson, P. E., Manivel, C., and Klang, D. T. (1989) *Hum. Pathol. 20*, 281−7.
15. Chaubert, P., and Hurlimann, J. (1992) *Arch. Pathol. Lab. Med. 116*, 1181−8.
16. Pagani, A., Sapino, A., Eusebi, V., Bergnolo, P., and Bussolati, G. (1994) *Virchows Arch. 425*, 459−65.
17. Losi, L., Lorenzini, R., Eusebi, G., and Bussolati, G. (1995) *Appl. Immunohistochem. 3*, 91−8.
18. Requena, L., Yus, E. S., Nunez, C., White, C. R., and Sangueza, O. P. (1996) *Am. J. Dermatopathol. 18*, 385−95.
19. Autiero, M., Gaubin, M., Mani, J. C., Castejon, C., Martin, M., El Marhomy, S., Guardiola, J., and Piatier-Tonneau, D. (1997) *Eur. J. Biochem. 245*, 208−13.
20. Veillette, A., Bookman, M. A., Horak, E. M., Samelson, L. E., and Bolen, J. B. (1989) *Nature 338*, 257−9.
21. Klatzmann, D., Champagne, E., Chamaret, S., Gruest, J., Guetard, D., Hercend, T., Gluckman, J. C., and Montagnier, L. (1984) *Nature 312*, 767−8.
22. Maddon, P. J., Dalgleish, A. G., McDougal, J. S., Clapham, P. R., Weiss, R. A., and Axel, R. (1986) *Cell 47*, 333−48.
23. Garzino, D. A., DeVico, A. L., and Gallo, R. C. (1998) *J. Clin. Immunol. 18*, 243−55.
24. Gaubin, M., Autiero, M., Basmaciogullari, S., Metivier, D., Mishal, Z., Culerrier, R., Oudin, A., Guardiola, J., and Piatier-Tonneau, D. (1999) *J. Immunol. 162*, 2631−8.
25. Frank, R. (1992) *Tetrahedron 48*, 9217−32.
26. Molina, F., Laune, D., Gougat, C., Pau, B., and Granier, C. (1996) *Pept. Res. 9*, 151−5.
27. Deen, C. D., McDougal, J. S., Inacker, R., Folena-Wasserman, G., Arthos, J., Rosenberg, J., Maddon, P. J., Axel, R., and Sweet, R. (1988) *Nature 331*, 82−4.
28. Traunecker, A., Schneider, J., Kiefer, H., and Karjalainen, K. (1989) *Nature 339*, 68−70.
29. Autiero, M., Houlgatte, R., Martin, M., Auffray, C., Guardiola, J., and Piatier-Tonneau, D. (1995) *Int. Immunol. 7*, 191−7.
30. Simmons, D., and Seed, B. (1988) *J. Immunol. 141*, 2797−800.
31. Sambrook, J., Fritsch, E. F., and Maniatis, T. (1989) *Molecular Cloning: A Laboratory Manual*, 2nd ed., Cold Spring Harbor Laboratory, Plainview, NY.
32. Malmqvist, M. (1993) *Nature 361*, 186−7.
33. Karlsson, R., and Falt, A. (1997) *J. Immunol. Methods 200*, 121−33.
34. Bergamo, P., Balestrieri, M., Cammarota, G., Guardiola, J., and Abrescia, P. (1997) *Hum. Immunol. 58*, 30−41.
35. Wong, P. Y., Staren, E. D., Tereshkova, N., and Braun, D. P. (1998) *J. Surg. Res. 76*, 95−103.
36. Kurt, R. A., Urba, W. J., Smith, J. W., and Schoof, D. D. (1998) *Int. J. Cancer 78*, 16−20.
37. Lopez, C. B., Rao, T. D., Feiner, H., Shapiro, R., Marks, J. R., and Frey, A. B. (1998) *Cell Immunol. 190*, 141−55.
38. Caputo, E., Autiero, M., Mani, J. C., Basmaciogullari, S., Piatier-Tonneau, D., and Guardiola, J. (1998) *Int. J. Cancer 78*, 76−85.
39. Caputo, E., Carratore, V., Ciullo, M., Tiberio, C., Mani, J. C., Piatier-Tonneau, D., and Guardiola, J. (1999) *Eur. J. Biochem 265*, 664−70.
40. Weiergraber, O., Schneider, M. J., Grotzinger, J., Wollmer, A., Kuster, A., Exner, M., and Heinrich, P. C. (1996) *FEBS Lett. 379*, 122−6.
41. Laune, D., Molina, F., Ferrieres, G., Mani, J. C., Cohen, P., Simon, D., Bernardi, T., Piechaczyk, M., Pau, B., and Granier, C. (1997) *J. Biol. Chem. 272*, 30937−44.

BI992398L